DOI: 10.1002/cphc.200600108

Specific Vectorial Immobilization of Oligonucleotide-Modified Yeast Cytochrome *c* on Carbon Nanotubes

Hendrik A. Heering,*[a, b] Keith A. Williams,[b] Simon de Vries,[c] and Cees Dekker[b]

Iso-1-cytochrome c *from the yeast* Saccharomyces cerevisiae *(YCC) contains a surface cysteine residue, Cys102, that is located opposite to the lysine-rich side containing the exposed heme edge, which is the docking site for enzymes. Site-specific vectorial immobilization of YCC via Cys102 on single-walled carbon nanotubes (SWNT) thus provides a selective interface between nanoscopic electronic devices and complex enzymes. We have achieved this by modification of Cys102 with an oligonucleotide (dT_{18}). Atomic force microscopy, fluorescence imaging, and cyclic voltammetry show the specific adsorption of YCC, modified with dT_{18}, on the SWNT sidewall with retention of its native properties. Pretreatment of the SWNT with Triton-X405 blocks the nonspecific binding of untreated YCC but does not interfere with binding of the oligonucleotide-modified YCC.*

Introduction

Carbon nanotubes are important materials for the fabrication of nanoscopic electrodes. Single-walled carbon nanotubes (SWNTs) have a well-defined cylindrical geometry, with a diameter in the nanometer range.[1] Recently, Heller et al.[2] demonstrated that individual SWNTs can be used as nanoelectrodes for electrochemistry. Devices were fabricated in which ≈ 1 μm of a SWNT sidewall was exposed to an aqueous solution of a ferrocene derivative, and cyclic voltammetry was performed. The nanoscopic dimensions led to a high current density at the electrode surface, allowing the study of both the fast heterogeneous electron-transfer kinetics at the nanotube sidewall, and redox enzyme kinetics that are not limited by mass transport. Advances in the bio-functionalization of SWNTs open a route towards electrochemical single-biomolecule studies.[3–11] The high conductivity pathway provided by SWNT has been successfully applied in macroscopic enzyme electrodes consisting of a vertically aligned carbon nanotube "forest".[4–7] Nanoscopic electrodes made from an individually contacted SWNT may allow innovative biological applications, such as the probing of local cellular environments and, ultimately, the measurement of the electrocatalytic activity of a single redox enzyme.

Since very few biomolecules—or even just a single one—may be present on such a small electrode, a strong, efficient, and (preferably) an orientationally specific immobilization of the biomolecules is of paramount importance. The durability of the device may be improved by optimizing the orientation of the enzyme for stability. Moreover, the vectorial immobilization of a redox enzyme is important to obtain a fast and well-defined electron-transfer pathway. This can be achieved by coupling a unique surface amino-acid residue, either directly or via a short spacer, to the electrode surface. Alternatively, not the enzyme itself but instead its natural redox partner protein can be adsorbed, provided that the docking site for the enzyme is facing the solution. Because many enzymes exchange electrons with small redox proteins, such as azurin, ferredoxin, and cytochrome *c*, such a device will have a broad applicability.

Mitochondrial cytochrome *c* has been shown to spontaneously adsorb on carbon nanotubes.[12–14] The interaction most likely occurs via the protein side that is rich in Lys residues, since the primary amines strongly bind to carboxylate functionalities,[15–19] and amines are also known to strongly interact with the carbon-nanotube sidewall.[20–22] Because the heme group slightly protrudes into the solution on that side, this orientation is very favorable for fast electron exchange. Unfortunately, the same Lys-rich side of cytochrome *c* is also the docking site for enzymes.[23–28] Such nonspecific adsorption will therefore hamper the interaction with the redox enzymes and thereby severely limit its utility. The application of cytochrome *c* as an intermediate between a carbon nanotube and a redox enzyme thus requires the modification of an amino-acid resi-

[a] *Dr. H. A. Heering*
Leiden Institute of Chemistry, Leiden University
Einsteinweg 55, 2333 CC Leiden (The Netherlands)
Fax: (+31) 71-5274349
E-mail: h.a.heering@chem.leidenuniv.nl

[b] *Dr. H. A. Heering, Prof. K. A. Williams,[+] Prof. C. Dekker*
Kavli Institute of Nanoscience, Delft University of Technology
Lorentzweg 1, 2628 CJ Delft (The Netherlands)

[c] *Prof. S. de Vries*
Department of Biotechnology, Delft University of Technology
Julianalaan 67, 2628 BC Delft (The Netherlands)

[+] *Current address:*
Department of Physics, University of Virginia
382 McCormick Road, Charlottesville, Virginia 22904 (USA)

due opposite to the heme cleft. Fortunately, iso-1-cytochrome *c* from the yeast *Saccharomyces cerevisiae* (YCC) contains a unique, naturally occurring surface cysteine residue. Notably, this Cys102 is located opposite to the lysine-rich side containing the exposed edge of the heme.[29] The properties of vectorially orientated YCC, chemisorbed via Cys102 at thiol-modified surfaces, have been extensively studied.[30–33] Scanning probe microscopy has shown that YCC can be immobilized directly on gold via Cys102.[34–36] Moreover, we have shown that YCC, vectorially chemisorbed on gold, exhibits very fast, reversible interfacial electron transfer and retains its native functionality, that is, the ability to interact with redox enzymes in solution. Electron relay via YCC is sufficiently fast to reveal mechanistic properties of these enzymes.[36]

The goal herein is to develop a method to vectorially immobilize YCC on a carbon-nanotube sidewall without introducing defects that would reduce the conductivity. The method will be suitable for applications to nanofabricated devices in which the electrode consists of a partially exposed SWNT. This will enable the fabrication of a biocompatible nanoscopic electrode with specific docking sites for a variety of unmodified redox enzymes. We demonstrate that YCC can be tethered to the sidewall of a SWNT via Cys102 with retention of its native properties. To achieve this, we modify the Cys102 thiol with an oligonucleotide and utilize the ability of oligonucleotides to form a strong, noncovalent complex with the sidewall of a carbon nanotube.[37] The addition of the surfactant Triton-X405 prevents the nonspecific adsorption of YCC.

Experimental Section

Materials: Iso-1-cytochrome *c* from YCC was purchased from Sigma. The phosphate buffer saline (PBS) consists of a solution of sodium phosphate (NaH_2PO4 and Na_2HPO_4 from Merck; 20 mM total phosphate) and NaCl (150 mM) at pH 7. Hepes buffer [*N*-(2-hydroxyethyl) piperazine-*N*-(2-ethanesulfonic acid), Sigma] was titrated to pH 7 with NaOH. The surfactant Triton-X405 was added from a 70% stock solution (Aldrich). Aqueous suspensions of carbon nanotubes were prepared by ultrasonicating SWNTs, produced by the high-pressure CO (HiPCO) method (provided by R. E Smalley, Rice University[38]) in 1% Triton-X405.[39] Deionized water (18 MΩ cm milli-Q, Millipore) was used to prepare all solutions and for rinsing the samples and electrodes.

Cytochrome *c* Modification: The dT_{18} oligonucleotide (50 μM), 3′-modified via a C_3 linker with an amine functionality (Isogen Bioscience) in PBS, was incubated for 30 min at room temperature with *m*-maleimidobenzoyl-*N*-hydroxysuccinimide ester [MBS, Pierce; 1 mM added from a 10 mM stock solution in dimethyl sulfoxide (DMSO)]. Excess unreacted MBS was subsequently removed by repeated filtration (three times), that is, dilution with buffer (PBS) and at least tenfold concentration over a 3 kDa cutoff filter (Microcon YM3, Amicon).

A solution of YCC (18 μM) in PBS was then incubated for one hour with this maleimide-3′-dT_{18} oligonucleotide (39 μM). Because in oxidized yeast cytochrome *c* the surface cysteine is not accessible due to dimerization, the modification was carried out in the presence of 1 mM tris[2-carboxyethyl]phosphine (TCEP, Pierce), which acted as a reductant. Excess unreacted oligonucleotide was subsequently removed by repeated dilution in PBS and concentration over a 10 kDa cutoff filter (Microcon YM10, Amicon), as described above, until the filtrate was free from oligonucleotide. To prevent nonspecific binding of the oligonucleotide to YCC, 0.5 M $MgSO_4$ (J. T. Baker) was added to the PBS buffer.

A portion of the dT_{18}-modified YCC (YCC–dT_{18}) was fluorescently labeled by incubating YCC–dT_{18} (10 μM) in PBS for one hour with the mono-succinimidyl ester of Cyanine3 (Cy3, Amersham Biosciences; 50 μM added from a 5 mM stock solution in DMSO). Unreacted Cy3 was separated from the product (Cy3–YCC–dT_{18}) by repeated dilution in PBS and concentration over a YM10 filter, as described above, until the filtrate was free from Cy3. The concentrations of cytochrome *c*, oligonucleotide, and Cy3, as well as the yield and integrity of the products, were determined by UV/Vis absorption spectroscopy (Jasco V-530 spectrophotometer).

Atomic Force Microscopy (AFM): The SWNTs were grown through chemical vapor deposition (CVD) from catalyst islands on a silicon wafer with a thermally grown oxide layer.[40] These devices are similar to those used by Heller et al. to fabricate SWNT sidewall electrodes.[2] The devices were incubated for 1 to 5 min with YCC or YCC–dT_{18} in PBS (with or without Triton-X405 in solution) or only with Triton-X405 in PBS, then thoroughly rinsed with water, dried under a stream of nitrogen, and mounted onto the atomic force microscope (Nanoscope IV, Digital Instruments). The images were recorded in the tapping mode, using silica cantilevers with a typical tip size of 10 nm (Olympus).

Fluorescence Microscopy: A suspension of HiPCO SWNTs (0.5 μg mL^{-1}) in Triton-X405 (0.05%) and Cy3–YCC–dT_{18} (0.1 μM) in PBS was incubated for one hour. Freshly cleaved mica (grade V-4, SPI supplies) was incubated with 0.01% poly-L-lysine (5–10 kDa, Fluka) for 20 s and then rinsed with water and dried under a stream of nitrogen. The modified nanotubes were deposited on this surface by applying the suspension for 20 s, followed by rinsing and drying. The samples were examined with a fluorescence microscope (Leica DMRXA) equipped with a spectrum analyzer (SpectraCube, Applied Spectral Imaging). Fluorescent images were obtained using optical filters, with excitation between 515 and 560 nm and detection of the emission above 560 nm. The emission spectrum of the fluorescent features was verified to be that of Cy3. The samples were also inspected with white light for structural features.

Electrochemistry: For measuring the reduction potential of (modified) YCC in solution, a 2 mm^2 gold disk was used as the working electrode (Bioanalytical Systems). The gold electrode was polished with a water-based diamond suspension (Buehler, 1 μm particles), rinsed, and then incubated for 30 min in 10 mM 6-mercapto-1-hexanol (Aldrich). A 10–25 μL droplet of solution (10 μM YCC or modified YCC in 20 mM Hepes with 0.5 M $MgSO_4$, pH 7) was placed between the working electrode, the reference electrode, and a platinum-wire counter electrode, as described by Hagen.[41] The cell was flushed with wetted nitrogen and connected to a Bioanalytical Systems CV-50W potentiostat for cyclic voltammetry. The reference electrode was a Ag/AgCl/3 M NaCl electrode (Bioanalytical Systems RE-5B, +215 mV versus the normal hydrogen electrode, NHE). All potentials are given versus the NHE. Carbon-nanotube electrodes were prepared from a suspension (≈1 mg mL^{-1}) of HiPCO SWNTs in ethanol. A droplet of the suspension was applied on a gold electrode and the solvent evaporated at 150 °C. This was repeated several times to obtain a uniform, dense layer of carbon nanotubes. The nanotube electrodes were then used in the setup described above.

Results and Discussion

Properties of YCC Modified with dT_{18}

Since poly-dT is known to strongly bind to the SWNT sidewall,[37] Cys102 is covalently attached via a short, bifunctional maleimide/succinimidyl linker to a dT_{18} oligonucleotide containing a 3′ amine. The ratio of dT_{18} to YCC is 1.03, as determined from the increase of the absorbance at 260 nm, using $\varepsilon_{547nm} = 29.5\,mM^{-1}cm^{-1}$ for reduced YCC, and $\varepsilon_{260nm} = 180.4\,mM^{-1}cm^{-1}$ for dT_{18}. The UV/Vis spectra in Figure 1 show

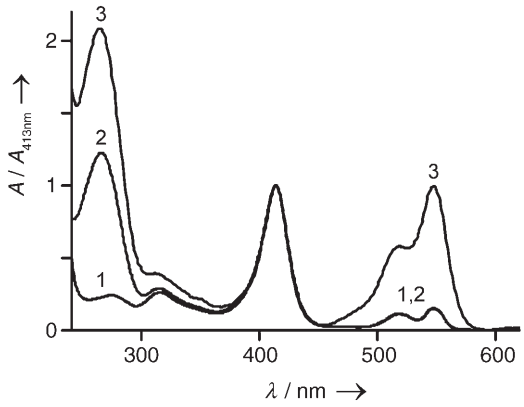

Figure 1. UV/Vis spectra (normalized to the Soret band at 413 nm) of reduced YCC (1), YCC–dT_{18} (2), and Cy3–YCC–dT_{18} (3) in PBS with 1 mM TCEP.

that the attachment of the dT_{18} oligonucleotide to Cys102 does not alter the spectroscopic properties of the heme. In addition, the reduction potentials of both unaltered YCC and YCC–dT_{18}, as determined by diffusion-controlled cyclic voltammetry with a mercaptohexanol-modified gold electrode, are both 280 mV at pH 7 (data not shown). This indicates that the modification does not alter the properties of YCC. The UV/Vis spectra and the reduction potentials are also not affected by the addition of 1% Triton-X405.

Atomic Force Microscopy

To prevent nonspecific binding of YCC on the carbon nanotubes, we tested the effect of Triton-X405 on the adsorption of YCC on basal-plane graphite. Preliminary AFM trials showed that YCC does adsorb from a 1 μM solution in PBS on bare basal-plane graphite. However, it adsorbs to a much lesser extent when the surface is pretreated with 1% Triton-X405 (data not shown). In addition, when 0.5% Triton-X405 was also present in the YCC solution, no features were observed anymore. We then incubated the carbon nanotubes on Si/SiO_2 with 0.5% Triton-X405 and 0.7 μM reduced YCC. As shown in Figure 2A, no YCC is present on either the nanotubes or the SiO_2 surface. However, if the device is subsequently incubated with 0.7 μM reduced YCC–dT_{18}, the nanotubes are clearly decorated with features (Figure 2B). The average height of these features is 2.6 nm relative to the nanotube height, which is

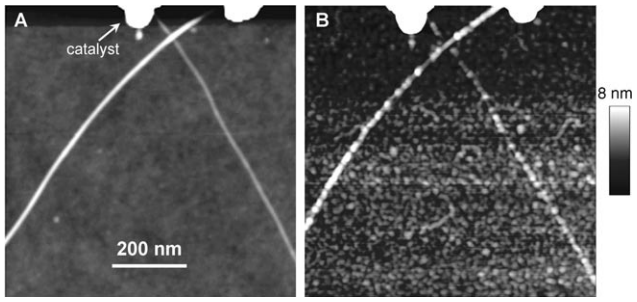

Figure 2. Tapping-mode AFM images of SWNTs grown on SiO_2, incubated with YCC in Triton-X405 and with YCC–dT_{18}: A) treated with 0.5% Triton-X405 and 0.7 μM YCC in PBS with 0.5 mM TCEP, and B) subsequently treated with 0.7 μM YCC–dT_{18} in PBS with 0.5 mM TCEP.

similar to the crystallographic diameter of YCC.[29] In addition, many features are also present on the SiO_2 surface.

To improve the selectivity for the nanotubes, we tested the effect of adding Triton-X405 to the YCC–dT_{18} solution. As shown in Figure 3, initially pretreating the device with Triton-

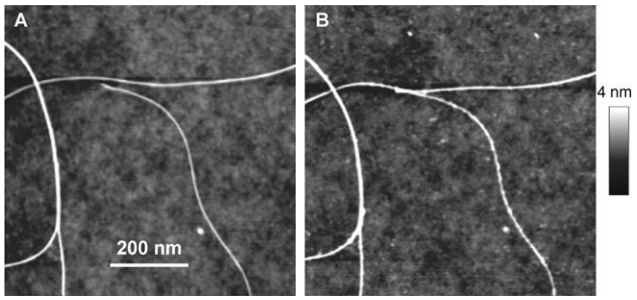

Figure 3. Tapping-mode AFM images of SWNTs on SiO_2 showing the effect of adding Triton-X405 to the YCC–dT_{18} solution A) treated with 0.1% Triton X405 in PBS with 1 mM TCEP, and B) subsequently treated with 1.3 μM YCC–dT_{18} in PBS with 1 mM TCEP and 0.1% Triton-X405.

X405 and then incubating it with 1.3 μM reduced YCC–dT_{18} in the presence of 0.1% Triton-X405 renders the adsorption highly specific for the carbon nanotube sidewalls. These results show that Triton-X405 effectively blocks the nonspecific interactions of YCC with the carbon nanotubes—and also with SiO_2—but does not interfere with the binding of the dT_{18} "tail" to the nanotube sidewalls. Poly-ethyleneglycol (PEG) is well known to block protein adsorption,[8] but Triton is required to fully coat carbon nanotubes with PEG.[11] Triton-X100 without PEG does not prevent cytochrome *c* adsorption on the SWNT,[12] despite the fact that it contains a short tail with ten PEG units. Our findings that Triton-X405 does block the nonspecific adsorption of YCC is most likely due to its four-times-longer PEG chain compared to Triton-X100.

Fluorescent Labeling

To confirm that the AFM features on top of the carbon nanotubes are indeed YCC molecules we labeled YCC–dT_{18} with the fluorescent dye Cy3. The ratio of Cy3 to YCC is 1.10, as deter-

mined from the increase of the absorbance at 548 nm, with $\varepsilon_{413nm} = 196\,mM^{-1}cm^{-1}$ for reduced YCC, and $\varepsilon_{548nm} = 150\,mM^{-1}cm^{-1}$ for Cy3. As shown in Figure 1, the heme Soret band at 413 nm in the UV/Vis absorption spectrum is comparable to that of unmodified YCC. Moreover, the reduction potential of this Cy3–YCC–dT_{18} construct, measured with cyclic voltammetry at a mercaptohexanol-modified gold electrode, is equal to that of untreated YCC (data not shown). This implies that the double modification of YCC with both Cy3 and dT_{18} does not significantly alter the electronic properties of the heme.

A suspension of $0.5\,mg\,L^{-1}$ carbon nanotubes in 0.05% Triton-X405 was incubated for one hour with 0.1 μM Cy3–YCC–dT_{18} in PBS (which corresponds to one YCC molecule per ≈3 nm of nanotube). These nanotubes were subsequently deposited on a mica surface that was pretreated with poly-lysine to immobilize the carbon nanotubes. Figure 4 shows a fluorescence image of the sample. The distribution of the fluorescent features suggests that the Cy3 labels are assembled on linear structures with a length of >2 μm. This arrangement does not coincide with either mica steps or other features on the surface, as verified by imaging with white backlighting. Incubation of the surface with 1 μM Cy3–YCC–dT_{18} only gives a featureless, uniform fluorescent background and incubation with bare carbon nanotubes in Triton-X405 does not yield any fluorescence. Hence, we conclude that the fluorescently labeled YCC–dT_{18} is immobilized on the sidewall of the nanotubes, supporting the assignment of the AFM features to YCC.

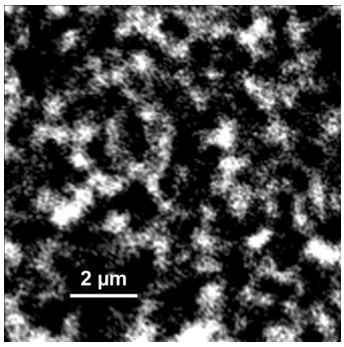

Figure 4. Fluorescence microscopy image of HiPCO SWNTs incubated with Cy3-labeled YCC–dT_{18} and deposited on poly-Lys-treated mica. The image is shown with a 30% intensity cutoff to eliminate background fluorescence.

Cyclic Voltammetry

The integrity of the immobilized YCC–dT_{18} construct and its ability to exchange electrons with the SWNT are assessed by voltammetry. A macroscopic electrode is required for obtaining a large enough YCC sample to yield detectable direct oxidation and reduction currents. We used an electrode consisting of a densely packed multilayer of carbon nanotubes to ensure that YCC–dT_{18} can only exchange electrons with the top-most layer of nanotubes and not with the underlying contact electrode. Firstly, the nanotube electrode was incubated with a 1% Triton-X405 solution for 1 min to block nonspecific binding of YCC. Then, it was incubated for 40 min with 0.75 μM YCC–dT_{18} in PBS and 0.1% Triton-X405, thoroughly rinsed, and measured in PBS with 1 M $MgSO_4$ (pH 7.0).

As shown in Figure 5A, a clear and reversible pair of peaks is observed at 269 (cathodic) and 289 mV (anodic) after incubation with YCC–dT_{18}. The integral of the peaks is 0.2 ± 0.04 μC, which corresponds to 2 pmol of adsorbed YCC. Considering the crystallographic dimensions of YCC,[29] this occupies a surface area of 11 mm^2, which is equivalent to a nearly full electroactive coverage on the upper-layer nanotubes (accounting for surface roughness). The background current of 11.2 μA at $50\,mV\,s^{-1}$ yields a capacitance of $32\,F\,m^{-2}$, compared to $0.9\,F\,m^{-2}$ for the bare gold electrode. The relatively large capacitance can be attributed to the larger surface area of the nanotube mesh probed by small ions, compared to that accessible to YCC–dT_{18}. The YCC peaks appear to be narrow for a one-electron reaction, but this is due to the restricted scan range used (140 mV). At a wider range, however, the characteristic carbon-electrode surface peaks at 168 (cathodic) and 316 mV (anodic) obscure the YCC response (Figure 5B). The small separation between the cathodic and anodic YCC peaks is comparable to the finite peak separation (not attributable to electron-transfer kinetics) observed for YCC directly chemisorbed via Cys102 on gold.[36] The midpoint potential of adsorbed YCC–dT_{18} is 279 mV, which is equal to that of YCC in solution. This implies that YCC–dT_{18} retains its native conformation, and that the heme group is outside the electric field emanating from the nanotubes.[42,43] This is consistent with tethering of YCC via Cys102–dT_{18} to the exposed upper layer of the dense nanotube mesh, with the heme cleft facing the solution.

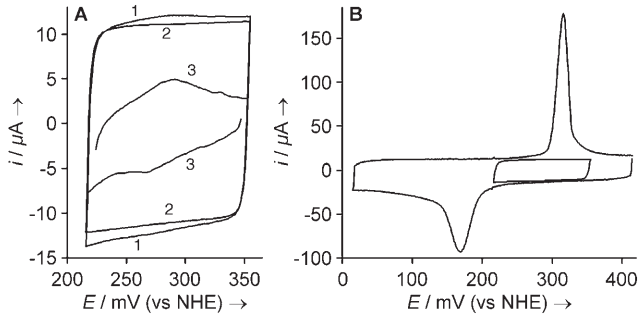

Figure 5. Voltammetry of YCC–dT_{18} adsorbed on a HiPCO SWNT multilayer electrode (geometric area 7 mm^2) in PBS buffer with 1 M $MgSO_4$ (scan rate: $50\,mV\,s^{-1}$). The electrode was pretreated with a 1% Triton-X405 solution, incubated with 0.75 μM YCC–dT_{18} in PBS and 0.1% Triton-X405, and rinsed. A) Voltammograms of YCC–dT_{18} (1), the recorded background (2), and the difference [(3); fivefold expanded]. B) Comparison of the voltammograms of YCC–dT_{18} at wide and narrow scan ranges.

Cyclic voltammetry thus demonstrates that oligonucleotide-modified YCC is able to bind to carbon nanotubes, with retention of its native properties, and to exchange electrons with them.

Conclusions

We have demonstrated that the sidewalls of the Triton-coated carbon nanotubes can only be decorated with YCC when Cys102 is modified with an oligonucleotide. Triton-X405 effectively prevents the nonspecific adsorption of unmodified YCC on the SWNT, but does not interfere with the oligonucleotide binding. Adsorption is apparent from AFM, as the carbon nanotubes are decorated with features with the expected height of YCC. When the carbon nanotubes are incubated with oligonucleotide-modified YCC, which is also labeled via Lys residues with the dye Cy3, fluorescent features are observed that can be assigned to Cy3 associated with the deposited nanotubes. Moreover, on a macroscopic carbon-nanotube-multilayer electrode, a voltammetric response is observed at the reduction potential of YCC. Therefore, the AFM features are assigned to YCC molecules that are vectorially immobilized at the SWNT sidewall via the oligonucleotide. Modification of Cys102 with an oligonucleotide does not alter the reduction potential or the spectroscopic properties of YCC. The redox properties are also not affected when this hybrid is bound to carbon nanotubes. Thus, cytochrome *c* can be specifically immobilized on the SWNT sidewall with retention of its native properties and in an orientation that allows for electron transfer and favors the interaction with the redox enzymes. Nanoscopic electrodes consisting of one YCC-modified SWNT are a significant step towards single-enzyme electrochemistry and applications in selective nanoscopic biosensor devices.

Acknowledgments

This work was financially supported by the Delft Interfaculty Research Center Life Science and Technology (DIOC LifeTech) and by the Netherlands Organization for Scientific Research (NWO). We thank Yuval Garini for providing the fluorescence microscope facility, and Iddo Heller and Jing Kong for providing devices with CVD-grown SWNT on Si/SiO2.

Keywords: biosensors · cytochrome *c* · immobilization · nanotubes · oligonucleotides

[1] C. Dekker, *Phys. Today* **1999**, *52*, 22 – 28.
[2] I. Heller, J. Kong, H. A. Heering, K. A. Williams, S. G. Lemay, C. Dekker, *Nano Lett.* **2005**, *5*, 137 – 142.
[3] J. J. Gooding, *Electrochim. Acta* **2005**, *50*, 3049 – 3060.
[4] E. Katz, I. Willner, *ChemPhysChem* **2004**, *5*, 1085 – 1104.
[5] X. Yu, D. Chattopadhyay, I. Galeska, F. Papadimitrakopoulos, J. F. Rusling, *Electrochem. Commun.* **2003**, *5*, 408 – 411.
[6] X. Yu, S. N. Kim, F. Papadimitrakopoulos, J. F. Rusling, *Mol. Biosyst.* **2005**, *1*, 70 – 78.
[7] J. J. Gooding, R. Wibowo, J. Liu, W. Yang, D. Losic, S. Orbons, F. J. Mearns, J. G. Shapter, D. B. Hibbert, *J. Am. Chem. Soc.* **2003**, *125*, 9006 – 9007.
[8] Y. Lin, S. Taylor, H. Li, K. A. S. Fernando, L. Qu, W. Wang, L. Gu, B. Zhou, Y.-P. Sun, *J. Mater. Chem.* **2004**, *14*, 527 – 541.
[9] K. Besteman, J.-O. Lee, F. G. M. Wiertz, H. A. Heering, C. Dekker, *Nano Lett.* **2003**, *3*, 727 – 730.
[10] K. A. Williams, P. T. M. Veenhuizen, B. G. de la Torre, R. Eritja, C. Dekker, *Nature* **2002**, *420*, 761 – 761.
[11] M. Shim, N. W. S. Kam, R. J. Chen, Y. Li, H. Dai, *Nano Lett.* **2002**, *2*, 285 – 288.
[12] B. R. Azamian, J. J. Davis, K. S. Coleman, C. B. Bagshaw, M. L. H. Green, *J. Am. Chem. Soc.* **2002**, *124*, 12664 – 12665.
[13] J. J. Davis, K. S. Coleman, B. R. Azamian, C. B. Bagshaw, M. L. H. Green, *Chem. Eur. J.* **2003**, *9*, 3732- 3739.
[14] N. W. S. Kam, H. J. Dai, *J. Am. Chem. Soc.* **2005**, *127*, 6021 – 6026.
[15] S. Song, R. A. Clark, E. F. Bowden, M. J. Tarlov, *J. Phys. Chem.* **1993**, *97*, 6564 – 6572.
[16] P. L. Edmiston, J. E. Lee, S.-S. Cheng, S. S. Saavedra, *J. Am. Chem. Soc.* **1997**, *119*, 560 – 570.
[17] P. Hildebrandt, D. H. Murgida, *Bioelectrochem.* **2002**, *55*, 139 – 143.
[18] K. Niki, W. R. Hardy, M. G. Hill, H. Li, J. R. Sprinkle, E. Margoliash, K. Fujita, R. Tanimura, N. Nakamura, H. Ohno, J. H. Richards, H. B. Gray, *J. Phys. Chem. B.* **2003**, *107*, 9947 – 9949.
[19] J. Zhou, J. Zheng, S. Jiang, *J. Phys. Chem. B.* **2004**, *108*, 17418 – 17424.
[20] J. Liu, M. J. Casavant, M. Cox, D. A. Walters, P. Boul, W. Lu, A. J. Rimberg, K. A. Smith, D. T. Colbert, R. E. Smalley, *Chem. Phys. Lett.* **1999**, *303*, 125 – 129.
[21] J. Kong, H. J. Dai, *J. Phys. Chem. B.* **2001**, *105*, 2890 – 2893.
[22] E. Valentin, S. Auvray, J. Goethals, J. Lewenstein, L. Capes, A. Filoramo, A. Ribayrol, R. Tsui, J.-P. Bourgoin, J.-N. Patillon, *Microelect. Eng.* **2002**, *61*, 491 – 496.
[23] H. Pelletier, J. Kraut, *Science* **1992**, *258*, 1748 – 1755.
[24] J. A. R. Worrall, U. Kolczak, G. W. Canters, M. Ubbink, *Biochemistry* **2001**, *40*, 7069 – 7076.
[25] C. Hunte, S. Solmaz, C. Lange, *Biochim. Biophys. Acta* **2002**, *1555*, 21 – 28.
[26] S. Döpner, P. Hildebrandt, F. I. Rosell, A. G. Mauk, M. von Walter, G. Buse, T. Soulimane, *Eur. J. Biochem.* **1999**, *261*, 379 – 391.
[27] V. A. Roberts, M. E. Pique, *J. Biol. Chem.* **1999**, *274*, 38051 – 38060.
[28] D. Flöck, V. Helms, *Proteins* **2002**, *47*, 75 – 85.
[29] G. V. Louie, G. D. Brayer, *J. Mol. Biol.* **1990**, *214*, 527 – 555.
[30] A. M. Edwards, K. Zhang, C. E. Nordgren, J. K. Blasie, *Biophys. J.* **2000**, *79*, 3105 – 3117.
[31] A. Tronin, A. M. Edwards, W. W. Wright, J. M. Vanderkooi, J. K. Blasie, *Biophys. J.* **2002**, *82*, 996 – 1003.
[32] L. L. Wood, S.-S. Cheng, P. L. Edmiston, S. S. Saavedra, *J. Am. Chem. Soc.* **1997**, *119*, 571 – 576.
[33] P. L. Edmiston, S. S. Saavedra, *Biophys. J.* **1998**, *74*, 999 – 1006.
[34] B. Bonanni, D. Alliata, A. R. Bizzarri, S. Cannistraro, *ChemPhysChem* **2003**, *4*, 1183 – 1188.
[35] A. G. Hansen, A. Boisen, J. U. Nielsen, H. Wackerbarth, L. Chorkendorff, J. E. T. Andersen, J. D. Zhang, J. Ulstrup, *Langmuir* **2003**, *19*, 3419 – 3427.
[36] H. A. Heering, F. G. M. Wiertz, C. Dekker, S. de Vries, *J. Am. Chem. Soc.* **2004**, *126*, 11103 – 11112.
[37] M. Zheng, A. Jagota, E. D. Semke, B. A. Diner, R. S. Mclean, S. R. Lustig, R. E. Richardson, N. G. Tassi, *Nature Mater.* **2003**, *2*, 338 – 342.
[38] M. J. Bronikowski, P. A. Willis, D. T. Colbert, K. A. Smith, R. E. Smalley, *J. Vac. Sci. Technol. A.* **2001**, *19*, 1800 – 1805.
[39] V. C. Moore, M. S. Strano, E. H. Haroz, R. H. Hauge, R. E. Smalley, J. Schmidt, Y. Talmon, *Nano Lett.* **2003**, *3*, 1379 – 1382.
[40] J. Kong, H. T. Soh, A. M. Cassell, C. F. Quate, H. J. Dai, *Nature* **1998**, *395*, 878 – 881.
[41] W. R. Hagen, *Eur. J. Biochem.* **1989**, *182*, 523 – 530.
[42] D. H. Murgida, P. Hildebrandt, *J. Phys. Chem. B* **2001**, *105*, 1578 – 1586.
[43] D. H. Murgida, P. Hildebrandt, *Phys. Chem. Chem. Phys.* **2005**, *7*, 3773 – 3784.

Received: April 19, 2006
Revised: May 1, 2006
Published online on June 28, 2006

